Task 1,4, and 5 are assisted or generated by Perplexity.AI, with the chatting history is available to review.

Task 1

(I) Working Principle

GNSS techniques for smartphone navigation, including Differential GNSS (DGNSS), Real-Time Kinematic (RTK), Precise Point Positioning (PPP), and PPP-RTK, will be compared in several aspects as follows.

1. **DGNSS**: Uses pseudorange measurements from a local base station to compute satellite signal errors (e.g., ionospheric and tropospheric delays). Corrections are broadcast to rovers via radio/internet, improving pseudorange-based positioning [1, 2].

2. **RTK**: Relies on pseudorange and carrier-phase measurements from both base and rover. Double-differencing eliminates common errors (orbital, atmospheric) to resolve integer ambiguities, enabling centimeter-level accuracy [2, 3].

3. **PPP**: Processes undifferenced pseudorange and carrier-phase measurements using precise satellite orbit/clock corrections from global networks. Models atmospheric delays internally [2, 4].

4. **PPP-RTK**: Combines PPP's global orbit/clock corrections with RTK-like regional atmospheric delay grids. Uses carrier-phase measurements and ambiguity resolution for faster convergence [4, 5].

(II) Level of Accuracy

Table 1: Level of accuracy for different GNSS techniques

Technique	Accuracy (Smartphone)
DGNSS	0.5–1 m
RTK	1-3 cm
PPP	5 cm
PPP-RTK	1-3 cm

(III) Supported Coverage

1. **DGNSS**: Local (50 km from base station).

2. **RTK**: Regional (10 km from base/CORS network).

3. **PPP**: Global (relies on satellite-broadcast corrections).

4. **PPP-RTK**: Regional (requires dense CORS network for atmospheric grids).

(IV) Robustness

1. **DGNSS/RTK**: Vulnerable to base-rover communication loss; multipath in urban canyons disrupts ambiguity resolution.

2. **PPP**: Resilient to local infrastructure failures but sensitive to correction data interruptions (e.g., internet loss).

3. **PPP-RTK**: Gracefully degrades to PPP accuracy if outside CORS coverage.

(V) Infrastructure and Cost

1. **DGNSS/RTK**: Require local base stations (high setup/maintenance costs) and real-time communication links.

2. **PPP**: Minimal infrastructure (global correction services like IGS), but subscription fees may apply.

3. **PPP-RTK**: Regional CORS networks balance cost and coverage; scalable for mass-market use.

(VI) Limitations

1. **DGNSS**: Accuracy limited by pseudorange noise and smartphone antenna quality; coverage restricted to base station proximity.

2. **RTK**: Performance degrades with baseline length; carrier-phase noise and multipath degrade performance in urban areas

3. **PPP**: Requires 10–20 minutes for decimeter-level accuracy.

4. **PPP-RTK**: Dependent on regional CORS density; smartphone antennas struggle with low carrier-phase SNR.

Finally, Table 2 briefly summarizes the properties of the four GNSS techniques for smartphone navigation [1, 2, 3, 4, 5].

Table 2: Summary on different GNSS techniques

Aspect	DGNSS	RTK	PPP	PPP-RTK
Measurements	Pseudorange	Pseudorange + carrier-phase	Pseudorange + carrier-phase	Pseudorange + carrier-phase
Accuracy	0.5–1 m	1-3 cm	5cm	1-3cm
Coverage	Local (50 km)	Regional (10 km)	Global	Regional (CORS)
Robustness	Link-dependent	Multipath-sensitive	Correction-dependent	Degrades to PPP
Infrastructure	Base station + link	CORS network	Global corrections	Global corrections + Regional CORS
Limitations	Vulnerable to pseudorange noise and antenna quality	Baseline constraints; High cost	Long convergence time	CORS dependency

Task 2

The given skymask dataset is the relationship between the azimuth angle (AZ_i ($i \in (1, 2, \ldots, 360)$)) and the corresponding lowest elevation angle (EL_i ($i \in (1, 2, \ldots, 360)$)) that enables Line-of-Sight (LOS) visibility. In the Ordinary Least-squares (OLS) positioning, each received satellite signal can be first determined with a certain

azimuth angle AZ_k ($k \in (1, 2, \ldots, 360)$), then if elevation angle given by the received satellite is lower than EL_k, we may assume it is not LOS observation and filter out this bad-quality measurement. At one epoch, after this skymask-filtering, if the available number of satellites is smaller than 4, we abort the positioning for this epoch. The above work procedures can be summarized in the flowchart in 1.
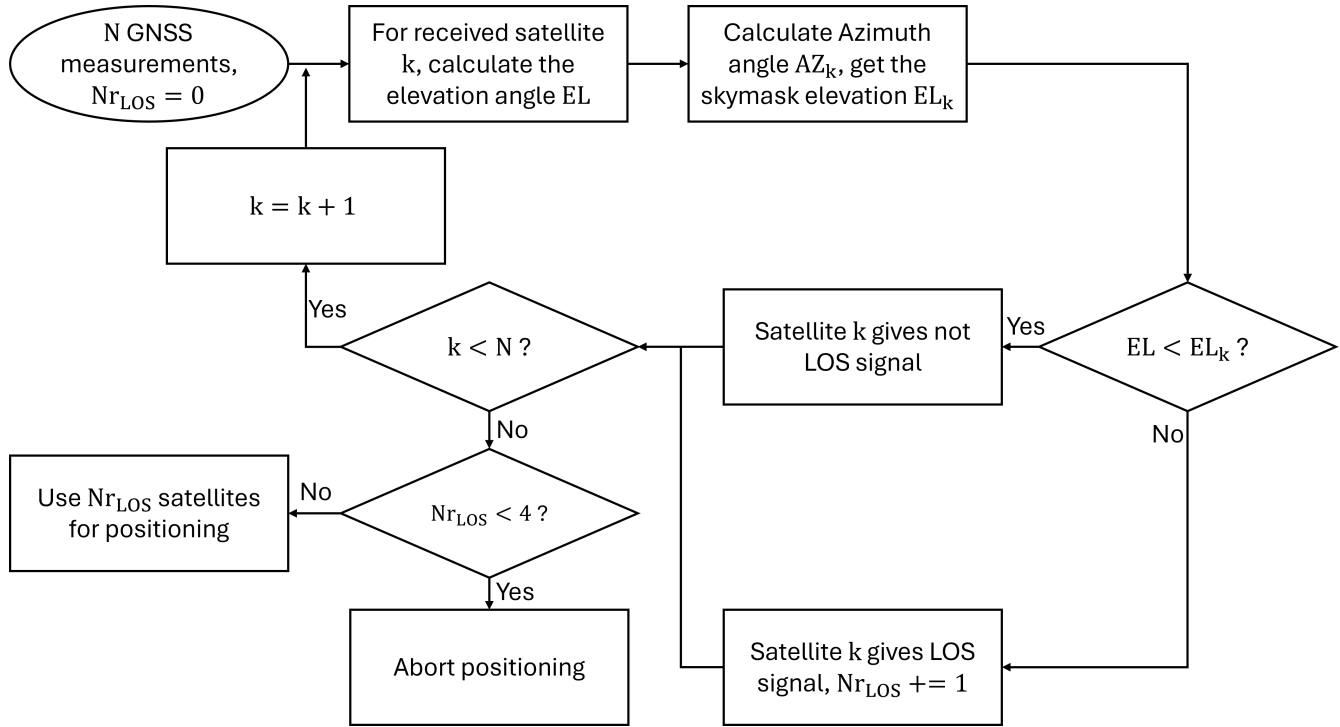

Figure 1: Workflow for skymask-filtering

As for the urban dataset with 839 epochs in total, the 2D positioning results of OLS with skymask and without skymask are summarized in Figure 2. It can be shown that the positioning precision is significantly improved because bad-quality measurements (i.e., not LOS signals) are filtered out. Table 3 also compares the standard deviation (STD) and root-mean-square error (RMSE) between the two methods. It can be shown that the positioning accuracy is not necessarily improved with skymask because the filtering process might result in less number of satellite signals for positioning. Notably, the skymask excludes the satellites based on the elevation angle, which is highly related their height information. Therefore, the geometry in the vertical dimension will be partly destroyed, thus generating worse 3D positioning performance. Besides, GNSS solutions exist in all the 839 epochs for both methods, which indicates 100% solution availability. However, theoretically, the skymask filtering scheme may not have sufficient number of LOS-signal satellites for least-squares estimation. Therefore, the OLS with skymask may not have solution for all the epochs.

Table 3: Comparison on 3D RMSE and STD between OLS and OLS with skymask-filtering

	3D RMSE (m)	3D STD (m)	Number of available epochs
OLS	85.13	35.33	839
OLS with skymask	100.36	33.18	839

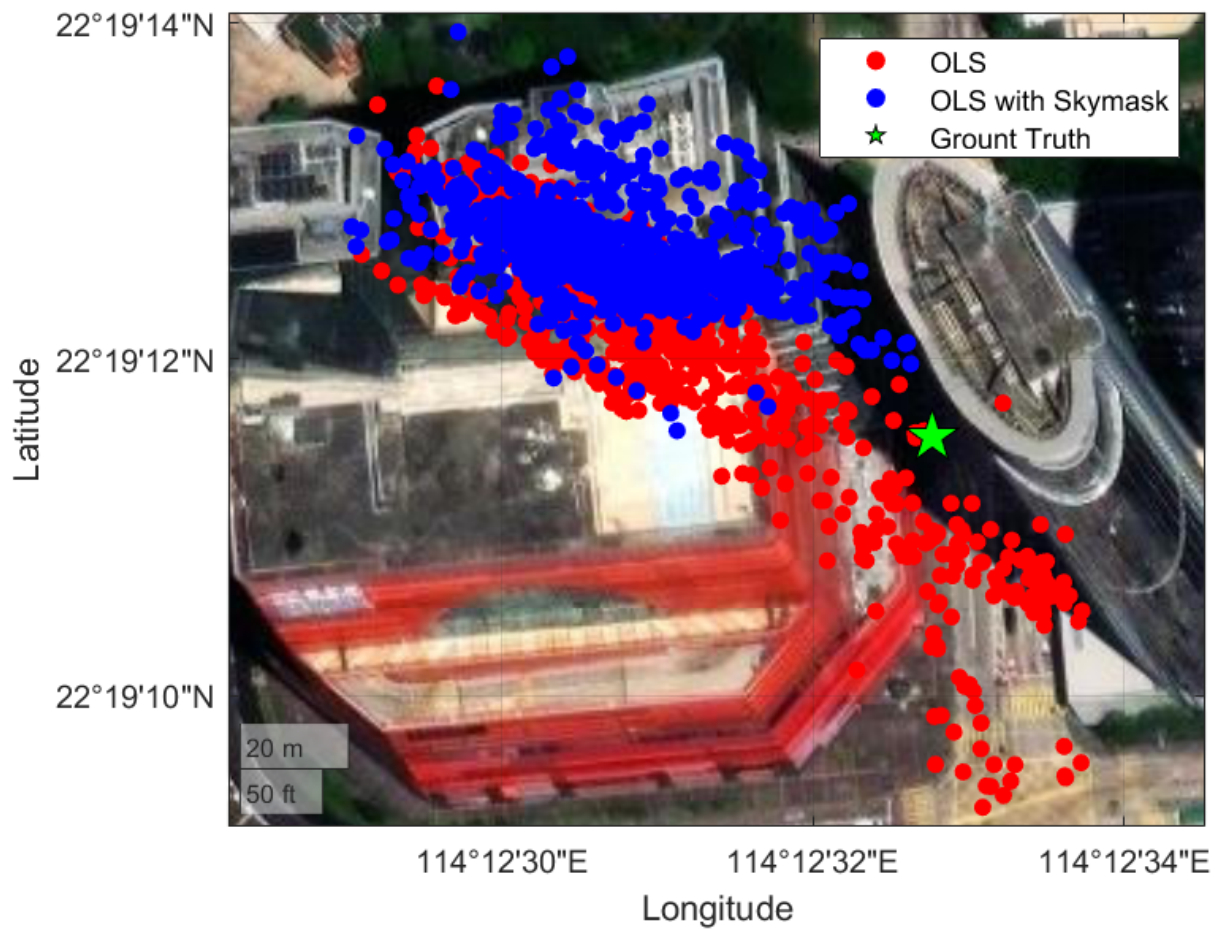Figure 2: 2D positioning comparison between OLS with and without skymask-filtering

Task 3

The following discussion will be conducted based on the "OpenSky" dataset, with 926 epochs in total. Throughout all the epochs, there are 9 received satellite signals. The RAIM scheme first considers detection, after which the isolation is conducted. If one single faulty measurement is detected, this specific measurement will be isolated and positioning will be conducted again.

In "*A2.m*", set *settings.sys.ls_type* = 1 to run WLS positioning. Line 154-189 in "*calcPosLSE.m*" implements the weighted RAIM along WLS, supported with functions "*chi2_detector.m*" and "*compute_PL.m*"

Consider the estimated weighted position $\boldsymbol{X}$ based on

$$\boldsymbol{X} = (\boldsymbol{G}^\top \boldsymbol{W} \boldsymbol{G})^{-1} \boldsymbol{G}^\top \boldsymbol{W} \boldsymbol{Y}, \tag{1}$$

the $WSSE$ test statistics is formulated as

$$WSSE = \sqrt{\boldsymbol{Y}^\top \boldsymbol{W}(\boldsymbol{I} - \boldsymbol{P})\boldsymbol{Y}}, \tag{2}$$

while the threshold T is given as:

$$T(N, P_{FA}) = \sqrt{Q_{\chi^2, N-4}(1 - P_{FA})}, \tag{3}$$

where $Q_{\chi^2, N-4}(\cdot)$ stands for the quantile function of Chi-square distribution with degree of freedom of $N - 4$. As for the protection level calculation, the 3-dimensional Pslope can be calculated for each satellite i:

$$\text{Pslope} = \frac{\sqrt{(K_{1,i}^2 + K_{2,i}^2 + K_{3,i}^2)}}{\sqrt{W_{ii}(1 - P_{ii})}}. \tag{4}$$

Combining Equation (3) and (4), the protection level (PL) for 3 dimensions can be calculated by:

$$\text{PL} = max[\text{Pslope}]T(N, P_{FA}) + k(P_{MD})\sigma, \tag{5}$$

where $\sigma = 3$m, and $k(P_{MD}) = Q_N\left(1 - \frac{P_{MD}}{2}\right)$ where $Q_N(\cdot)$ is the quantile function of standard normal distribution [6].

The classic RAIM and weighted RAIM are conducted for the OLS and WLS positioning results, respectively, and the results are shown in Figure 3. In Figure 3a, subfigure (1) shows that some epochs generate values of test statistic (blue curve) higher than the calculated threshold (red curve), which indicates possible faults. After detecting the epochs with faults, it is found that two possible faulty measurements always exist among the received signals during the isolation stage, so we cannot successfully isolate a single fault from the 9 measurements for those epochs. As a result, positioning during those epochs is aborted and there are no PL calculations, correspondingly (as shown in subfigure (2)). The subfigure (3) shows that all the PLs are below Alert limit (AL) of 50m. The above also confirms the effectiveness of our developed RAIM to detect and exclude faulty or low-quality measurements.

In Figure 3b, subfigure (1) shows all the test statistics during the 926 epochs are below the calculated threshold. Processed by the weighting scheme, no epoch in the WLS positionings is detected to possibly have faulty measurements, then no isolation procedure is conducted. PL can be calculated for all the epochs, as shown in subfigure (2). The Stanford chart in subfigure (3) shows that all the PL is within AL.

Task 4

Low Earth Orbit (LEO) satellites have emerged as a promising augmentation or alternative to traditional Global Navigation Satellite Systems (GNSS), offering stronger signals and improved positioning in challenging environments. However, integrating LEO satellites into GNSS navigation systems involves several complex challenges.
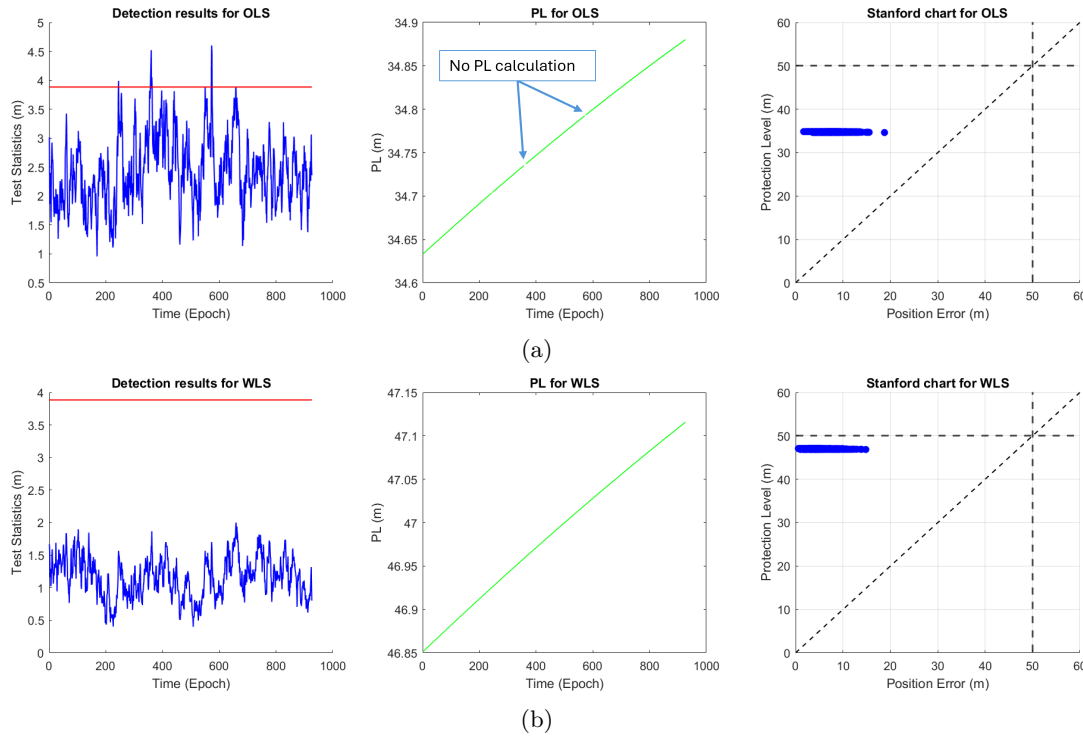
Figure 3: Subfigures (1) Comparison between threshold and test; (2) calculated PLs; (3) Standford chart, for (a) OLS and (b) WLS, where 'OLS' stands for Ordinary Least Squares algorithm

This report systematically discusses the key difficulties related to orbit and clock determination, integration with existing GNSS, coverage and constellation size, signal diversity and complexity, and vulnerability to jamming and spoofing.

1. **Orbit and Clock Determination**: One of the foremost challenges in LEO-based navigation is the precise determination of satellite orbits and clock parameters, which are fundamental for accurate positioning. Unlike GNSS satellites that are equipped with highly stable atomic clocks and have well-characterized orbits, LEO satellites typically use less stable oscillators such as Oven-Controlled Crystal Oscillators (OCXOs) or Ultra-Stable Oscillators (USOs) to reduce cost, weight, and power consumption [7, 8]. This results in increased clock noise and systematic errors that degrade timing precision.

   Real-time precise orbit determination (POD) for LEO satellites is complicated by their rapid orbital motion and the high volume of observation data that must be downlinked and processed. Although centimeter-level orbit accuracy can be achieved in post-processing, real-time processing faces discontinuities and data incompleteness due to downlink strategies and the sensitivity of clock precision to the quality of GNSS real-time products. Clock stability in LEO satellites is further affected by mid- to long-term systematic effects, with 10-minute predictions already incurring errors on the order of decimeters [8]. Strategies to mitigate these issues include enhancing dynamic orbit models, improving thermal control to reduce hardware biases, and potentially equipping LEO satellites with chip-scale atomic clocks [7].

   The development of inter-satellite links among LEO satellites shows promise for onboard real-time POD and clock synchronization, which could alleviate some ground segment dependencies. However, establishing a dedicated infrastructure for continuous orbit and clock broadcasting remains a significant operational challenge.

2. **Integration with Existing GNSS**: Integrating LEO satellite signals with traditional GNSS constellations is critical for realizing a robust, multi-layered navigation system. This integration requires tight time and

frequency synchronization between LEO and GNSS satellites to ensure compatibility and interoperability [9]. Unlike GNSS, which operates with a well-established time reference and navigation message formats, LEO constellations often lack standardized navigation data and rely on GNSS for orbit and clock determination, complicating seamless integration [9].

Moreover, the heterogeneous nature of LEO signals—varying in frequency bands, modulation schemes, and signal structures—poses challenges for receiver design and data fusion algorithms [9]. Effective integration demands advanced filtering and estimation techniques to combine LEO Doppler-based observables with GNSS pseudorange and carrier-phase measurements, balancing the strengths and weaknesses of each system.

The integration also involves harmonizing correction data and reference frames, as LEO satellites contribute additional observations that can improve GNSS orbit and clock products but require sophisticated joint processing frameworks. Ensuring that user devices can process multi-constellation signals efficiently without excessive power consumption or computational overhead remains an ongoing research focus.

3. **Coverage and Constellation Size**: Due to their low orbital altitude (typically 300–1500 km), LEO satellites have a much smaller instantaneous coverage footprint compared to Medium Earth Orbit (MEO) GNSS satellites. To guarantee continuous global coverage and sufficient satellite visibility for navigation, very large constellations—often numbering in the hundreds of satellites—are necessary. This requirement raises significant deployment, operational, and cost challenges [8].

The smaller footprint also means that users experience rapid changes in satellite geometry, which can be both an advantage (improving dilution of precision and reducing convergence times) and a challenge (increasing the complexity of tracking and maintaining continuous navigation solutions). The need for a dense constellation complicates constellation management, collision avoidance, and spectrum allocation [10].

Furthermore, the orbital inclination and distribution of LEO satellites affect coverage quality in polar and equatorial regions. While LEO constellations can improve positioning in traditionally underserved polar regions where GNSS coverage is limited, ensuring uniform global performance requires careful constellation design and continuous replenishment.

4. **Signal Diversity and Complexity**: LEO satellites transmit signals across multiple frequency bands (L, S, Ku, etc.) with diverse modulation schemes, often designed primarily for communication rather than navigation. This diversity complicates receiver design, as smartphones and other user devices must be capable of blind acquisition, tracking, and decoding of unfamiliar and proprietary signals.

The lack of standardized navigation messages and the variability in signal structures demand flexible and adaptive signal processing algorithms. Additionally, the high Doppler shifts induced by the rapid motion of LEO satellites require robust Doppler compensation and frequency tracking mechanisms. These factors increase receiver complexity, power consumption, and cost [9].

Moreover, the coexistence of communication and navigation signals within the same LEO constellation raises challenges related to interference management and signal prioritization, which must be addressed to maintain reliable PNT services.

5. **Vulnerability to Jamming and Spoofing**: While LEO satellites benefit from stronger signal power at the receiver due to their proximity, potentially enhancing resistance to jamming compared to GNSS, the proliferation of LEO constellations introduces new security concerns [11]. The large number of satellites and their diverse signal types increase the attack surface for malicious interference and spoofing.

Ensuring the authenticity and integrity of LEO navigation signals requires the development of advanced cryptographic protections and anti-spoofing techniques tailored to the unique characteristics of LEO signals. Additionally, the rapid satellite movement and frequent handovers between satellites complicate continuous authentication and anomaly detection.

The integration of LEO signals with GNSS also necessitates coordinated security frameworks to prevent cross-system spoofing attacks that could degrade the overall navigation solution.

Task 5

Global Navigation Satellite System Reflectometry (GNSS-R) is an innovative remote sensing technique that leverages the reflection of GNSS signals off the Earth's surface to extract valuable environmental information. Unlike traditional GNSS applications focused on positioning and timing, GNSS-R exploits the properties of reflected signals—such as power, delay, Doppler shift, and polarization changes—to characterize surface conditions. This technology has rapidly expanded its scope, offering impactful applications across oceanography, agriculture, climate monitoring, and disaster management. However, the deployment and operationalization of GNSS-R face several technical and methodological challenges that must be addressed to fully realize its potential.

Main Applications and Underlying Principles

At its core, GNSS-R operates as a bistatic radar system using existing GNSS signals transmitted from satellites like GPS, Galileo, GLONASS, and BeiDou. These signals illuminate the Earth's surface and are reflected toward receivers located on ground stations, airborne platforms, or satellites in Low Earth Orbit (LEO). By cross-correlating the reflected signals with either a locally generated replica or the directly received signal, GNSS-R produces Delay-Doppler Maps (DDMs), which spatially map the reflected signal power as a function of time delay and Doppler frequency shift. The shape and intensity of these DDMs encode surface properties such as roughness, moisture content, and dielectric constant [12].

1. **Ocean and Atmospheric Monitoring**: One of the earliest and most mature applications of GNSS-R is ocean surface monitoring. The inverse correlation between reflected signal power and ocean surface roughness enables the estimation of sea surface wind speed and wave height. NASA's CYGNSS mission, a constellation of eight microsatellites dedicated to GNSS-R, exemplifies this application by providing near real-time monitoring of tropical cyclones and hurricanes, leveraging the L-band GNSS signals' insensitivity to rain and clouds [13]. This capability significantly enhances meteorological forecasting and maritime safety.

2. **Land Surface and Cryosphere Applications**: GNSS-R has also proven effective for terrestrial remote sensing, including soil moisture estimation, surface inundation mapping, vegetation monitoring, and snow/ice thickness measurement. For instance, the Indian EOS-08 satellite's GNSS-R instrument has demonstrated high-resolution soil moisture retrieval over arid regions like the Sahara and surface inundation detection in the Amazon rainforest, achieving spatial resolutions better than 1 km. In polar regions, GNSS-R measurements of reflected signals through multi-layer ice provide insights into ice thickness changes, contributing to climate change assessments [14].

3. **Disaster Management and Environmental Monitoring**: The all-weather, passive nature of GNSS-R makes it particularly valuable for natural disaster monitoring. It enables the detection of floods, storm surges, and oil spills, offering near real-time situational awareness crucial for emergency response. Additionally, GNSS-R supports sustainable agriculture by providing soil moisture data that optimize irrigation and improve crop yields, aligning with global sustainability goals [14].

Impact of GNSS-R on These Applications

GNSS-R's impact lies in its ability to transform ubiquitous GNSS signals into a versatile environmental sensing tool without the need for dedicated transmitters, reducing cost and complexity. The technique's global coverage, high temporal sampling enabled by satellite constellations, and insensitivity to atmospheric conditions position it as a complementary technology to traditional remote sensing methods like Synthetic Aperture Radar (SAR) and radiometry. Its scalability, demonstrated by emerging CubeSat implementations, promises democratized access to high-quality environmental data.

Furthermore, GNSS-R leverages existing GNSS infrastructure and signals, which enhances cost-effectiveness and operational sustainability. The generation of Delay-Doppler Maps and normalized bistatic radar cross-sections (NBRCS) provides quantitative parameters that can be integrated into climate models, hydrological forecasts, and ecosystem monitoring frameworks, thereby advancing scientific understanding and practical applications alike.

Challenges and Limitations

Despite its transformative potential, GNSS-R faces several challenges that limit its current operational maturity and widespread adoption.

1. **Signal Processing Complexity**: Extracting meaningful geophysical parameters from reflected GNSS signals is non-trivial due to the weak signal strength, multipath effects, and the complex interaction of signals with heterogeneous surfaces. The generation and interpretation of Delay-Doppler Maps require sophisticated algorithms capable of discriminating between direct and reflected signals, mitigating noise, and compensating for varying reflection geometries. Advances in signal processing and machine learning are actively being pursued to enhance parameter retrieval accuracy [12, 15].

2. **Receiver Design and Calibration**: GNSS-R demands specialized receivers capable of simultaneously tracking direct and reflected signals across multiple GNSS constellations and frequency bands. Designing compact, low-power, multi-frequency receivers that can operate on spaceborne platforms or small satellites remains a technical hurdle. Precise calibration and validation against in situ measurements are essential to ensure data reliability, yet such ground truth datasets are limited in many regions [15].

3. **Spatial and Temporal Resolution Constraints**: Although GNSS-R can achieve resolutions on the order of 1 km over land and 15 km over oceans, these are coarser than some active remote sensing techniques. The spatial resolution depends on the geometry of the reflection zone and satellite-receiver configuration, which can limit the detection of small-scale features. Temporal resolution depends on satellite constellation size and revisit frequency, which are improving but still constrain real-time monitoring capabilities [16].

4. **Environmental and Atmospheric Effects**: Variability in surface roughness, vegetation cover, and soil texture complicates the interpretation of reflected signals. Additionally, ionospheric and tropospheric conditions can introduce phase and amplitude distortions that require correction. The dynamic nature of these environmental factors necessitates adaptive models and continuous algorithm refinement [12].

5. **Integration with Other Remote Sensing Systems**: To maximize utility, GNSS-R data must be integrated with complementary remote sensing datasets (e.g., SAR, radiometry, optical imagery). Harmonizing data formats, temporal and spatial scales, and uncertainty quantification across sensors is a complex but necessary endeavor for comprehensive Earth system monitoring [15].

References

[1] D. Sharp, "What are the Different GNSS Correction Methods? | Swiftnav." [Online]. Available: https://www.swiftnav.com/resource/blog/what-are-the-different-gnss-correction-methods

[2] C. Zang, "Differences between RTK and PPP." [Online]. Available: https://tersus-gnss.com/tech_blog/-Differences-between-RTK-and-PPP

[3] J. Hu, P. Li, and S. Bisnath, "Towards GNSS ambiguity resolution for smartphones in realistic environments: Characterization of smartphone ambiguities with RTK, PPP, and PPP-RTK," in *Proceedings of the 36th International Technical Meeting of the Satellite Division of The Institute of Navigation (ION GNSS+ 2023)*, 2023, pp. 2698–2711. [Online]. Available: https://www.ion.org/publications/abstract.cfm?articleID=19285

[4] P. Hou, J. Zha, T. Liu, and B. Zhang, "Recent advances and perspectives in GNSS PPP-RTK," *Measurement Science and Technology*, vol. 34, no. 5, p. 051002, May 2023. [Online]. Available: https://iopscience.iop.org/article/10.1088/1361-6501/acb78c

[5] P. Felts, "Network RTK vs PPP-RTK: An insight into real-world performance," Feb. 2024. [Online]. Available: https://www.u-blox.com/en/blogs/tech/network-rtk-vs-ppp-rtk

[6] R. G. Brown, G. Y. Chin, and J. H. Kraemer, "RAIM: Will It Meet the RTCA GPS Minimum Operational Performance Standards?" in *Proceedings of the 1991 National Technical Meeting of The Institute of Navigation*, 1991, pp. 103–111. [Online]. Available: https://www.ion.org/publications/abstract.cfm?articleID=5020

[7] A. El-Mowafy, K. Wang, and A. Allahvirdizadeh, "LEO aiding GNSS positioning in challenging environments," *XXVII FIG Congress*, 2022.

[8] A. El-Mowafy, K. Wang, Y. Li, and A. Allahvirdi-Zadeh, "THE IMPACT OF ORBITAL AND CLOCK ERRORS ON POSITIONING FROM LEO CONSTELLATIONS AND PROPOSED ORBITAL SOLUTIONS," *The International Archives of the Photogrammetry, Remote Sensing and Spatial Information Sciences*, vol. XLVIII-1/W2-2023, pp. 1111–1117, Dec. 2023. [Online]. Available: https://isprs-archives.copernicus.org/articles/XLVIII-1-W2-2023/1111/2023/

[9] FLORIAN. KUNZI, BENJAMIN. BRAUN, MARKUS. MARKGRAF, and OLIVER. MONTENBRUCK, "First Steps Toward a Fully Operational LEO PNT Payload - Inside GNSS - Global Navigation Satellite Systems Engineering, Policy, and Design," 2024. [Online]. Available: https://insidegnss.com/first-steps-toward-a-fully-operational-leo-pnt-payload/

[10] A. El-Mowafy, K. Wang, and A. Allahvirdizadeh, "The potential of LEO mega-constellations in aiding GNSS to enable positioning in challenging environments," *XXVII FIG Congress*, 2022.

[11] Y. Yang, Y. Mao, X. Ren, X. Jia, and B. Sun, "Demand and key technology for a LEO constellation as augmentation of satellite navigation systems," *Satellite Navigation*, vol. 5, no. 1, p. 11, Apr. 2024. [Online]. Available: https://doi.org/10.1186/s43020-024-00133-w

[12] G. Resources, "What is GNSS Reflectometry? How Does GNSS Reflectometry Work? Understanding Its Principles and Applications - GIS Resources," 2024. [Online]. Available: https://gisresources.com/what-is-gnss-reflectometry-how-does-gnss-reflectometry-workunderstanding-its-principles-and-applications/

[13] "GNSS Reflectometry." [Online]. Available: https://ggos.org/item/gnss-reflectometry/

[14] "New GNSS reflectometry system revolutionizes environmental remote sensing," 2025. [Online]. Available: https://www.oulu.fi/en/news/new-gnss-reflectometry-system-revolutionizes-environmental-remote-sensing

[15] S. Jin, A. Camps, Y. Jia, F. Wang, M. Martin-Neira, F. Huang, Q. Yan, S. Zhang, Z. Li, K. Edokossi, D. Yang, Z. Xiao, Z. Ma, and W. Bai, "Remote sensing and its applications using GNSS reflected signals: Advances and prospects," *Satellite Navigation*, vol. 5, no. 1, p. 19, Dec. 2024. [Online]. Available: https://satellite-navigation.springeropen.com/articles/10.1186/s43020-024-00139-4

[16] T. A. Johansen, "GNSS-R: Maritime Surveillance using GNSS-Reflectometry - NTNU," 2025. [Online].
      Available: https://www.ntnu.edu/smallsat/gnss-r-maritime-surveillance-using-gnss-reflectometry